



**HAL**  
open science

**Nonenzymatic oxygenated metabolites of  $\alpha$ -linolenic acid B1- and L1-phytoprostanes protect immature neurons from oxidant injury and promote differentiation of oligodendrocyte progenitors through PPAR- $\gamma$  activation.**

Luisa Minghetti, Rachele Salvi, Lavinia Salvatori Maria, Maria Antonietta Ajmone-Cat, Chiara de Nuccio, Sergio Visentin, Valérie Bultel-Poncé, Camille Oger, Alexandre Guy, Jean-Marie Galano, et al.

► **To cite this version:**

Luisa Minghetti, Rachele Salvi, Lavinia Salvatori Maria, Maria Antonietta Ajmone-Cat, Chiara de Nuccio, et al.. Nonenzymatic oxygenated metabolites of  $\alpha$ -linolenic acid B1- and L1-phytoprostanes protect immature neurons from oxidant injury and promote differentiation of oligodendrocyte progenitors through PPAR- $\gamma$  activation.. Free Radical Biology and Medicine, 2014, 73, pp.41-50. 10.1016/j.freeradbiomed.2014.04.025 . hal-01058083

**HAL Id: hal-01058083**

**<https://hal.science/hal-01058083v1>**

Submitted on 3 Jun 2021

**HAL** is a multi-disciplinary open access archive for the deposit and dissemination of scientific research documents, whether they are published or not. The documents may come from teaching and research institutions in France or abroad, or from public or private research centers.

L'archive ouverte pluridisciplinaire **HAL**, est destinée au dépôt et à la diffusion de documents scientifiques de niveau recherche, publiés ou non, émanant des établissements d'enseignement et de recherche français ou étrangers, des laboratoires publics ou privés.

# Nonenzymatic oxygenated metabolites of $\alpha$ -linolenic acid B<sub>1</sub>- and L<sub>1</sub>-phytoprostanes protect immature neurons from oxidant injury and promote differentiation of oligodendrocyte progenitors through PPAR- $\gamma$ activation

Luisa Minghetti<sup>a,\*</sup>, Rachele Salvi<sup>a</sup>, Maria Lavinia Salvatori<sup>a,1</sup>, Maria Antonietta Ajmone-Cat<sup>a</sup>, Chiara De Nuccio<sup>a</sup>, Sergio Visentin<sup>a</sup>, Valérie Bultel-Poncé<sup>b</sup>, Camille Oger<sup>b</sup>, Alexandre Guy<sup>b</sup>, Jean-Marie Galano<sup>b</sup>, Anita Greco<sup>a</sup>, Antonietta Bernardo<sup>a</sup>, Thierry Durand<sup>b</sup>

<sup>a</sup> Department of Cell Biology and Neuroscience, Istituto Superiore di Sanità, 00161 Rome, Italy

<sup>b</sup> Institut des Biomolécules Max Mousseron, UMR 5247 CNRS, UM I, UM II, ENSCM, Montpellier, France

## ABSTRACT

Phytoprostanes (PhytoP's) are formed in higher plants from  $\alpha$ -linolenic acid via a nonenzymatic free radical-catalyzed pathway and act as endogenous mediators capable of protecting cells from damage under various conditions related to oxidative stress. Humans are exposed to PhytoP's, as they are present in relevant quantities in vegetable food and pollen. The uptake of PhytoP's through the olfactory epithelium of the nasal mucosa, upon pollen grain inhalation, is of interest as the intranasal pathway is regarded as a direct route of communication between the environment and the brain. On this basis, we sought to investigate the potential activities of PhytoP's on immature cells of the central nervous system, which are particularly susceptible to oxidative stress. In neuroblastoma SH-SY5Y cells, used as a model for undifferentiated neurons, B<sub>1</sub>-PhytoP's, but not F<sub>1</sub>-PhytoP's, increased cell metabolic activity and protected them from oxidant damage caused by H<sub>2</sub>O<sub>2</sub>. Moreover, B<sub>1</sub>-PhytoP's induced a moderate depolarization of the mitochondrial inner membrane potential. These effects were prevented by the PPAR- $\gamma$  antagonist GW9662. When SH-SY5Y cells were induced to differentiate toward a more mature phenotype, they became resistant to B<sub>1</sub>-PhytoP activities. B<sub>1</sub>-PhytoP's also influenced immature cells of an oligodendroglial line, as they increased the metabolic activity of oligodendrocyte progenitors and strongly accelerated their differentiation to immature oligodendrocytes, through mechanisms at least partially dependent on PPAR- $\gamma$  activity. However, B<sub>1</sub>-PhytoP's did not protect oligodendrocyte progenitors against oxidant injury. Taken together, these data suggest that B<sub>1</sub>-PhytoP's, through novel mechanisms involving PPAR- $\gamma$ , can specifically affect immature brain cells, such as neuroblasts and oligodendrocyte progenitors, thereby conferring neuroprotection against oxidant injury and promoting myelination.

## Keywords:

Myelin  
Neuroblasts  
Neuroprotection  
Oligodendrocytes  
Oxidative stress  
Progenitors  
Fatty acids  
Free radicals

**Abbreviations:** AA, arachidonic acid; ALA,  $\alpha$ -linolenic acid; bFGF, basic fibroblast growth factor; CV, crystal violet; DHA, docosahexaenoic acid; IsoP, isoprostane; MAP2, microtubule-associated protein 2; mMP, mitochondrial inner membrane potential; MTT, 3-(4,5-dimethylthiazol-2-yl)-2,5-diphenyltetrazolium bromide; NeuroP, neuroprostane; OL, oligodendrocyte; OP, oligodendrocyte progenitor; PDGF, platelet growth factor; PhytoP, phytoprostane; PPAR- $\gamma$ , peroxisome proliferator-activated receptor  $\gamma$ ; PUFA, polyunsaturated fatty acid; RA, retinoic acid; TMRE, tetramethylrhodamine ethyl ester perchlorate

\* Corresponding author. Fax: +39 06 4957821.

E-mail address: [luisa.minghetti@iss.it](mailto:luisa.minghetti@iss.it) (L. Minghetti).

<sup>1</sup> Present address: Department of Biomedicine and Prevention, University "Tor Vergata," Rome, Italy.

Free radical-catalyzed oxidation of polyunsaturated fatty acids (PUFAs)<sup>2</sup> is a hallmark of oxidative stress. Arachidonic acid (AA; C20:4 $\omega$ 6) and docosahexaenoic acid (DHA; C22:6 $\omega$ 3) are the most abundant PUFAs in mammals, and their peroxidated products— isoprostanes (IsoP's) and neuroprostanes (NeuroP's), respectively— are considered among the most sensitive and reliable biomarkers of oxidative stress [1,2]. IsoP's and NeuroP's are large families of regio- and stereoisomeric prostaglandin-like molecules; some of them have been shown to display significant biological activities that could contribute to as well as protect from oxidant injury.

A third biologically active lipid family is represented by phytoprostanes (PhytoP's), which are formed in plants via a nonenzymatic

free radical-catalyzed pathway analogous to that leading to IsoP and NeuroP formation [3]. The PhytoP precursor is  $\alpha$ -linolenic acid (ALA; C18:3 $\omega$ 3), a predominant PUFA in higher plants, generally lacking the enzymatic capacity to form longer chain PUFAs such as AA and DHA. Several classes of PhytoP's are constitutively present in plants and their levels rise in response to oxidative stress [4]. As their counterparts in the animal kingdom, PhytoP's occur in several classes, named according to the prostaglandin classification, each of which can be generated as two racemic regioisomers (for further details see [5] and Fig. 1). The development of a new chemical strategy, based on a furan approach, has led to the synthesis of enantiomerically pure B<sub>1</sub>-, F<sub>1</sub>-, and E<sub>1</sub>-PhytoP's [6,7], thus allowing the full assessment of the biological activities of each of these compounds.

Among the best studied PhytoP's are those of the A and B classes. Several lines of evidence indicate that A<sub>1</sub>- and B<sub>1</sub>-PhytoP's in plant cells influence the expression of numerous genes, most of which are involved in the detoxification of xenobiotics and in cytoprotective responses, suggesting that B<sub>1</sub>-PhytoP's represent endogenous mediators capable of counteracting cell damage (see [8] and references therein). Much less is known of the potential biological activities of PhytoP's in mammalian systems.

Humans are potentially exposed to PhytoP's. Vegetable foods, in particular vegetable oils, contain high levels of ALA, which could be converted into PhytoP's by autoxidation during cooking and/or storage or after oral consumption in the gastrointestinal tract. Karg et al. [9] have shown that PhytoP's of the A<sub>1</sub>, B<sub>1</sub>, E<sub>1</sub>, and F<sub>1</sub> classes are present in up to milligram quantities per 100 ml in fresh

vegetable oil, with the highest levels found in linseed and soybean oils. These levels may further increase by more than an order of magnitude with storage, reaching submillimolar concentrations. After oral ingestion, PhytoP's are adsorbed and found in plasma and urine in conjugate and free form, respectively. Plasma and urinary levels of F<sub>1</sub>-PhytoP's were found increased in healthy men after 4 weeks of flaxseed oil supplementation compared to a control group receiving olive oil supplementation [10]. PhytoP's have also been detected in parenteral lipid nutrition used in intensive care medicine, containing lipid fractions from vegetable oils such as soybean and olive oils [10].

In addition to oral ingestion, humans can be exposed to PhytoP's through inhalation of pollen, rich in both ALA and PhytoP's. Upon contact with the respiratory mucosa, pollen grains release allergens in conjunction with many other substances, including bioactive lipids, collectively called pollen-associated lipid mediators. Aqueous pollen extracts contain significant levels of E<sub>1</sub>-, F<sub>1</sub>-, A<sub>1</sub>-, and B<sub>1</sub>-PhytoP's. Of these, E<sub>1</sub>-PhytoP is among the most prominent and it has been identified as one of the pollen-associated lipid mediators, capable of modulating dendritic cell functions and favoring a type 2-dominated proallergic immune response [11,12]. The fact that PhytoP's can be released from pollen grains upon contact with the airway mucosa, and in particular nasal mucosa, is intriguing as the intranasal pathway is regarded as a direct route of communication between the environment and the brain.

In addition to the above-mentioned immunomodulatory activity of E<sub>1</sub>-PhytoP on human dendritic cells, few other PhytoP biological

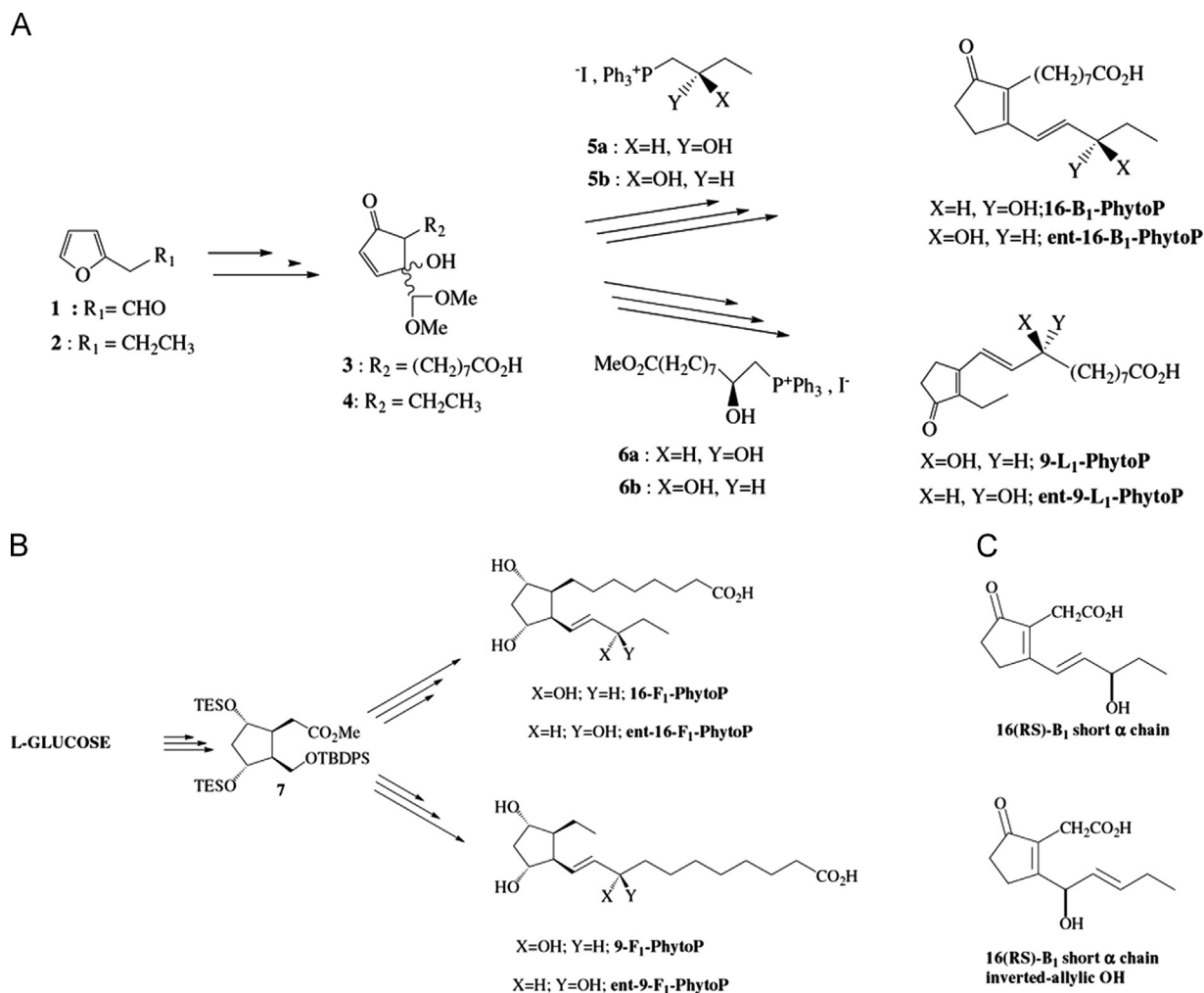


Fig. 1. Total synthesis of F<sub>1</sub>-, B<sub>1</sub>-, and L<sub>1</sub>-PhytoP's and analogs. See Materials and methods for details.

activities on animal systems have been reported. A<sub>1</sub>- and B<sub>1</sub>-PhytoP's have been shown to inhibit the release of nitric oxide in lipopolysaccharide-stimulated RAW264.7 macrophages, whereas in leukemia Jurkat T cells A<sub>1</sub>- but not B<sub>1</sub>-PhytoP's trigger apoptosis [9].

Taken together, these observations suggest that PhytoP's are bioactive lipids in both plant and animal systems and highlight the importance of better understanding their potential biological roles, in particular with respect to oxidative stress [11].

On this basis we sought to investigate the possible effects of B<sub>1</sub>- and F<sub>1</sub>-PhytoP's on immature cells of the central nervous system, which are particularly susceptible to oxidative stress. As experimental models we used SH-SY5Y cells, a cell line derived from a human neuroblastoma and resembling neuroblasts [13], and primary cultures of rat oligodendrocyte (OL) progenitors (OPs) [14]. To induce oxidant injury, cells were exposed to hydrogen peroxide (H<sub>2</sub>O<sub>2</sub>). We show that B<sub>1</sub>-PhytoP's protect SH-SY5Y cells against oxidant injury through mechanisms involving activation of the nuclear receptor peroxisome proliferator-activated receptor (PPAR)- $\gamma$ . In these cells, B<sub>1</sub>-PhytoP's induce a moderate depolarization of the mitochondrial inner membrane potential (mMP), which is also dependent on PPAR- $\gamma$  activation and could be part of the defensive response triggered by B<sub>1</sub>-PhytoP's. Upon differentiation, SH-SY5Y cells become resistant to B<sub>1</sub>-PhytoP activities. Similarly, B<sub>1</sub>-PhytoP's do not protect OPs against oxidant injury but they strongly accelerate OP differentiation to immature OLs. Again, B<sub>1</sub>-PhytoP-induced OL differentiation was at least partially dependent on PPAR- $\gamma$  activity.

## Materials and methods

### *Synthesis of phytosteranes*

The two regioisomers 16-B<sub>1</sub>- and 9-L<sub>1</sub>-PhytoP, previously known as PPB<sub>1</sub> type I and type II (Fig. 1A), were prepared by total synthesis according to our published procedures [15]. Briefly, the 3-hydroxy-4-cyclopentenone key intermediates (3 and 4, Fig. 1A) in our furan strategies were obtained from the commercially available furfural and *n*-propylfuran (1 and 2, Fig. 1A) in seven and five steps, respectively, with good yields. The introduction of the  $\alpha$  and  $\omega$  chains of PhytoP's bearing the hydroxyl allylic chiral center was achieved using chiral phosphonium salts (5 and 6, Fig. 1A). The synthesis of the 16-F<sub>1</sub>- and 9-F<sub>1</sub>-PhytoP's (Fig. 1B) was achieved using our earlier strategy based on a radical cyclization step, starting from commercially available *l*-glucose as chiral pools [6].

### *Cell cultures*

Human SH-SY5Y neuroblastoma cells (ATCC, Manassas, VA, USA) were cultured in 1/1 Dulbecco's modified Eagle's medium (DMEM; Lonza, Milan, Italy)/Ham's F12 medium (Cambrex Bio Science-Verviers, Verviers, Belgium) supplemented with 10% fetal bovine serum, 1 mM *L*-glutamine, and antibiotics 50 U/ml penicillin and 50  $\mu$ g/ml streptomycin (Invitrogen, Eugene, OR, USA). Cell cultures were maintained in a 5.0% CO<sub>2</sub> humidified atmosphere at 37 °C and split at about 80% confluence for a maximum of 20 passages. Cells were harvested by trypsinization and the cell suspension was resuspended in fresh medium and seeded at a density of 10<sup>5</sup> cells/cm<sup>2</sup> in 96-well plates (BD Falcon, Franklin Lakes, NJ, USA), for 3-(4,5-dimethyl thiazol-2-yl)-2,5-diphenyl tetrazolium bromide (MTT) or crystal violet (CV) assay, or 6-well plates for Western blot or plated on glass coverslips (Steroglass, Perugia, Italy) for video imaging or immunocytochemistry experiments. Cell differentiation was induced by exposing SH-SY5Y cells, after 24 h of plating, to 5  $\mu$ M retinoic acid (RA; Sigma, St. Louis,

MO, USA) in complete growth medium. The cells were maintained under these conditions for 5 days with medium change every 2 days.

Purified cultures of OPs were prepared from newborn Wistar rats as described [14] and in accordance with the European Communities Council Directive No. 86/609/EEC. OPs growing on top of mixed glial monolayers were mechanically detached and seeded at the density of 6  $\times$  10<sup>4</sup> cells/cm<sup>2</sup> into poly-*L*-lysine-coated 35-mm-diameter plastic culture dishes or 96-well plates. At 2 h after plating, the culture medium (DMEM with high glucose, supplemented with 10% fetal calf serum) was replaced with a chemically defined serum-free medium, consisting of DMEM/Ham's F12 (4/1) supplemented with 5.6 mg/ml glucose, 5  $\mu$ g/ml insulin, 100  $\mu$ g/ml human transferrin, 100  $\mu$ g/ml bovine serum albumin, 0.06 ng/ml progesterone, 40 ng/ml sodium selenite, 16  $\mu$ g/ml putrescine, bFGF, PDGF, 50 U/ml penicillin, 50  $\mu$ g/ml streptomycin, and 2 mM glutamine. All supplements were from Sigma. After 24 h, the cells were exposed to several conditions as detailed in the figure legends.

### *MTT and crystal violet assays*

The ability of cells to reduce MTT (Sigma) was assessed as an index of cellular metabolic activity and mitochondrial integrity, as previously described [14]. MTT was added at a final concentration of 0.25 mg/ml during the final 4 h of incubation. The medium was then removed, and 100  $\mu$ l of dimethyl sulfoxide (DMSO) was added to each well to dissolve the dark blue crystals. The plates were then read on a microplate reader, using a test wavelength of 570 nm and a reference wavelength of 630 nm. The cell number in each condition was estimated by CV dye [18]. Protein concentration was measured by BCA protein assay (Thermo/Pierce, Rockford, IL, USA).

### *Determination of mitochondrial membrane potential*

To measure mitochondrial membrane potential we used the potentiometric dye tetramethylrhodamine ethyl ester perchlorate (TMRE; Sigma) at a final concentration of 30 nM (from 1 mM stock solution in DMSO). Cells were kept for 30 min (OPs) or 50 min (SH-SY5Y cells) in the presence of TMRE before recording, to reach saturation of the dye, and maintained throughout the entire experiment to avoid the decay of the signal. An oil immersion objective (Olympus; 40 $\times$ , 1.35 NA) mounted on an inverted microscope (Axiovert 135; Carl Zeiss, Oberkochen Germany) was utilized for fluorescence video imaging. The excitation wavelength 535 nm was applied by means of a monochromator (Till Photonics, Polychrome II, Munich, Germany) and the emission light at 590 was collected by a CCD, cooled digital camera (PCO, Sensicam, Kelheim, Germany) and recorded. The Imaging Workbench 6.0 software package (Indec BioSystems, Santa Clara, CA, USA) was used for recording and offline analysis of the data. The software allowed the measurement of the emission value in regions of interest or along line profiles, where peaks of amplitude corresponded to single mitochondria. The average amplitudes of the fluorescence intensity were calculated (from a minimum of three experiments for each condition) and shown in bar graphs as the average  $\pm$  SEM, with *n* representing the number of observations.

### *Immunofluorescence*

SH-SY5Y cells were fixed in 4% paraformaldehyde and permeabilized (0.2% Triton X-100/phosphate-buffered saline (PBS)). After a blocking step in 3% bovine serum albumin (BSA) Triton X-100/PBS, the cells were incubated with rabbit anti-MAP2 polyclonal antibodies (1:500 in 3% BSA/PBS) 2 h at room temperature. After

being rinsed, the cells were incubated with Cy3 donkey anti-rabbit (Jackson ImmunoResearch Laboratories, West Grove, PA, USA; 1:200) in PBS, 1 h at room temperature. Nuclei were stained using Hoechst 33258 (5 µg/ml for 20 min, Sigma, Italy). Coverslips were then mounted with DAKO fluorescence mounting medium.

OPs were incubated with the oligodendroglial marker O<sub>4</sub>, by using a primary monoclonal antibody (mouse immunoglobulin M (IgM), hybridoma supernatants; diluted 1:5) and, as secondary antibody, fluorescein-conjugated goat anti-mouse IgM (1:200, Jackson ImmunoResearch Laboratories), before fixation in 4% paraformaldehyde. For PPAR-γ translocation, cells were incubated overnight at 4 °C with anti-PPAR-γ polyclonal rabbit antibodies (1:100; Calbiochem, San Diego, CA, USA) and processed with secondary antibodies as before. Coverslips were mounted with Vectashield mounting medium (Vector Laboratories, Burlingame, CA, USA) and examined using a Leica DM4000B fluorescence microscope equipped with a DFC420C digital camera and Leica Application Suite software (260RI) for image acquisition. Cells were counted in 10 microscopic fields of 0.18 mm<sup>2</sup> per coverslip prepared in duplicate for each condition from at least three independent experiments.

### Statistical analysis

Data are expressed as means ± SEM of *n* independent experiments (run in duplicate). Statistical significance was evaluated using Student's *t* test or one-way ANOVA for multiple comparisons. Numbers of independent experiments are indicated in the figure legends; *p* < 0.05 was accepted as statistical significance. Analyses were performed using Stata 8.1 software (Stata Corp., College Station, TX, USA).

## Results

### *B*<sub>1</sub>- but not *F*<sub>1</sub>-phytosteranes enhance SH-SY5Y cell metabolic activity

The human neuroblastoma SH-SY5Y cell line is widely used as a model cell system for studying neuronal death induced by oxidative stress and, in particular, H<sub>2</sub>O<sub>2</sub>-induced oxidant injury [16]. We first examined the effects of 16-*B*<sub>1</sub>-PhytoP, 9-*L*<sub>1</sub>-PhytoP, and 9- and 16-*F*<sub>1</sub>-PhytoP's (Fig. 1A and B) on cell viability. SH-SY5Y cells were exposed for 24 h to the various PhytoP's (0.1–10 µM), and cell viability was examined by MTT reduction assay. 16-*B*<sub>1</sub>-PhytoP and 9-*L*<sub>1</sub>-PhytoP increased the ability of SH-SY5Y cells to reduce MTT, whereas 16-*F*<sub>1</sub>-PhytoP and 9-*F*<sub>1</sub>-PhytoP had no effect (Fig. 2A), suggesting that the *B*<sub>1</sub> cyclopentenone ring, but not the *F*<sub>1</sub> cyclopentane ring, is important for PhytoP activity on SH-SY5Y cells. On this basis we focused our study on the *B*<sub>1</sub> series.

MTT reduction assay is based on the ability of living cells to take up MTT and to reduce it by NADH-dependent dehydrogenases and it is generally used as a measure of cell viability. To verify whether the *B*<sub>1</sub>-PhytoP-induced increase in MTT reduction was due to an enhanced metabolic activity or, rather, to cell proliferation, we evaluated the cell number using CV, a dye that binds to DNA. As shown in Fig. 2B, there was no difference between 16-*B*<sub>1</sub>-PhytoP- and 9-*L*<sub>1</sub>-PhytoP-treated and untreated cultures, suggesting that both 16-*B*<sub>1</sub>-PhytoP and 9-*L*<sub>1</sub>-PhytoP types increase cell metabolic activity rather than cell proliferation.

As opposed to 16-*B*<sub>1</sub>-PhytoP, the cyclopentenone isoprostane (15-*A*<sub>2t</sub>-IsoP), an oxidized arachidonic acid metabolite, induced a significant cell impairment, when tested at comparable concentration range (Fig. 2C), as previously described in primary hippocampal neurons [17].

To gain more information on the relation between biological activity and chemical structure, we tested the 16-*B*<sub>1</sub>-PhytoP and

9-*L*<sub>1</sub>-PhytoP enantiomers (Fig. 1A) and two *B*<sub>1</sub>-PhytoP derivatives characterized by a short side chain and alternative allylic alcohol migration, as depicted in Fig. 1C. Of the four compounds, only *ent*-16-*B*<sub>1</sub>-PhytoP induced a significant increase in MTT reduction, when tested at high concentration (25 µM, Fig. 3A). Altogether, these results suggest that allylic configuration and the position of the carboxyl group with respect to the cyclopentenone ring are two important factors controlling the *B*<sub>1</sub>-PhytoP biological profile.

### *16-B*<sub>1</sub>-PhytoP and *9-L*<sub>1</sub>-PhytoP protect undifferentiated SH-SY5Y cells against oxidant injury

We next examined whether PhytoP's could protect SH-SY5Y cells against H<sub>2</sub>O<sub>2</sub>-induced oxidant injury. Cells were exposed to increasing concentrations of H<sub>2</sub>O<sub>2</sub> to identify the concentration yielding an approximately 50% cell impairment, as assessed by MTT reduction assay (Fig. 4A). On the basis of this dose-response curve, cells were then exposed to 0.25 mM H<sub>2</sub>O<sub>2</sub> alone or in combination with 16-*B*<sub>1</sub>-PhytoP, 9-*L*<sub>1</sub>-PhytoP, or their enantiomers, at two concentrations (10 and 25 µM). Both 16-*B*<sub>1</sub>-PhytoP and 9-*L*<sub>1</sub>-PhytoP prevented the H<sub>2</sub>O<sub>2</sub>-dependent cell impairment. As before, of the two enantiomers, only *ent*-16-*B*<sub>1</sub>-PhytoP showed a protective activity, at both concentrations tested (Fig. 4B).

Undifferentiated SH-SY5Y cells are neuroblast-like cells that can acquire a functional neuron-like phenotype in response to treatment with various agents, including RA. Because differentiation is known to be associated with changes in susceptibility to both neurotoxins and neuroprotective substances [18], we tested the biological activity of 16-*B*<sub>1</sub>-PhytoP and 9-*L*<sub>1</sub>-PhytoP on SH-SY5Y cells after differentiation. To this aim, SH-SY5Y cells were exposed to 5 µM RA added to the culture medium at days 1 and 3, according to Miglio et al. [19]. At day 5, compared to control cultures, RA-treated cells showed a neuron-like morphology and higher expression of microtubule-associated protein 2 (MAP2), a protein associated with microtubules of differentiated neurons (Fig. 5A). Differentiated SH-SY5Y cells were exposed to H<sub>2</sub>O<sub>2</sub> and or PhytoP's at day 4 for 24 h. As shown in Fig. 5C, differentiated SH-SY5Y cells were less sensitive to H<sub>2</sub>O<sub>2</sub>-induced oxidant injury compared to the undifferentiated cells, and 0.5 mM concentration was required to obtain an approximately 40% impairment. When differentiated cells were challenged with 16-*B*<sub>1</sub>-PhytoP, 9-*L*<sub>1</sub>-PhytoP, or the inactive *ent*-9-*L*<sub>1</sub>-PhytoP, alone or in combination with 0.5 mM H<sub>2</sub>O<sub>2</sub> (Fig. 5D), none of the three compounds affected MTT reduction by themselves or rescued cells from H<sub>2</sub>O<sub>2</sub> toxicity, suggesting that the biological activities of *B*<sub>1</sub>-PhytoP's on neuronal cells are dependent on their differentiation state.

### *16-B*<sub>1</sub>-PhytoP protects undifferentiated SH-SY5Y cells through PPAR-γ-mediated mechanisms

A mechanism of action proposed for PhytoP's, in particular *E*<sub>1</sub>-PhytoP's, is the activation of the nuclear receptor PPAR-γ. To assess whether this receptor was mediating *B*<sub>1</sub>-PhytoP protective activity on undifferentiated SH-SY5Y cells, we focused on 16-*B*<sub>1</sub>-PhytoP. SH-SY5Y cells were challenged with H<sub>2</sub>O<sub>2</sub> and 16-*B*<sub>1</sub>-PhytoP, alone or in the presence of the specific PPAR-γ antagonist GW9662 (Fig. 6A). The antagonist did not modify per se the toxic activity of H<sub>2</sub>O<sub>2</sub> but it prevented the protective effect of 16-*B*<sub>1</sub>-PhytoP, indicating that PPAR-γ activation is necessary for the protection against H<sub>2</sub>O<sub>2</sub>-induced oxidant injury.

Several lines of evidence indicate that in plants 16-*B*<sub>1</sub>-PhytoP and 9-*L*<sub>1</sub>-PhytoP may influence the expression of adaptive-response genes, enabling cells to counteract cell damage caused by various toxicants and, in particular, those causing oxidative stress. PPAR-γ is a ligand-dependent transcription factor regulating the expression of several target genes, including antioxidant enzymes such as catalase and Cu/Zn-superoxide dismutase. However, we did not observe any

effect of 16-B<sub>1</sub>-PhytoP expression on these enzymes after 24 h of treatment (not shown).

A potentially important mechanism for promoting cellular protection against oxidant stress is a slight degree of depolarization of the inner membrane of mitochondria [20]. To examine if this was the case in 16-B<sub>1</sub>-PhytoP-treated SH-SY5Y cells, we used the potentiometric dye TMRE in single-cell video-imaging experiments to measure the changes in mMP in cells exposed for 24 h to either 16-B<sub>1</sub>-PhytoP or the inactive *ent*-9-L<sub>1</sub>-PhytoP. The intensities of the TMRE fluorescence signal were decreased only in cells treated with 16-B<sub>1</sub>-PhytoP (Fig. 6B). As for the protective effect against H<sub>2</sub>O<sub>2</sub> toxicity, the presence of the PPAR-γ antagonist GW9662 abolished the decrease in mMP caused by 16-B<sub>1</sub>-PhytoP, without affecting the mMP of untreated cells (Fig. 6C).

*16-B<sub>1</sub>-PhytoP and 9-L<sub>1</sub>-PhytoP do not protect oligodendrocyte progenitors but promote their differentiation*

OPs are highly susceptible to oxidant injury and represent a target of oxidative stress in the brain. OPs, isolated from mixed glial cultures, were grown in chemically defined medium in the presence of growth factors (bFGF and PDGF) for 24 h before addition of 16-B<sub>1</sub>-, 9-L<sub>1</sub>-, or *ent*-9-L<sub>1</sub>-PhytoP's. Cell viability was

tested after 24 h (2 days in vitro cultures, 2 DIV) by MTT assay. Of the three compounds, only 16-B<sub>1</sub>-PhytoP significantly increased the ability of OPs to reduce MTT (Fig. 7A). However, in the presence of 0.025 or 0.05 mM H<sub>2</sub>O<sub>2</sub> (giving a reduction of about 20 and 50% of cell viability, respectively), 16-B<sub>1</sub>-PhytoP, tested at two concentrations (1 and 10 μM), was unable to prevent or mitigate cell impairment (Fig. 7B). Interestingly, the 24-h exposure of OPs to 1 μM 16-B<sub>1</sub>-PhytoP, but not to *ent*-9-L<sub>1</sub>-PhytoP, promoted OP maturation as indicated by the increased number of cells expressing O<sub>4</sub>, a marker for immature OLs (Fig. 8A). In addition, compared to control cultures, 16-B<sub>1</sub>-PhytoP-treated cultures exhibited a more complex and branched morphology, another hallmark of oligodendrocyte differentiation (Fig. 7B). The effect on morphology was more evident after 72 h of exposure to 16-B<sub>1</sub>-PhytoP (Fig. 8B, 4 DIV).

Neither 16-B<sub>1</sub>-PhytoP nor *ent*-9-L<sub>1</sub>-PhytoP significantly affected mitochondrial membrane potential in OP cultures exposed for 24 h to the compounds (Fig. 8C). However, as in the case of protection in SH-SY5Y cells, the effect of 16-B<sub>1</sub>-PhytoP in OP cultures was at least in part due to PPAR-γ activation. As shown in Fig. 8D, the presence of the specific PPAR-γ antagonist GW9662 partially prevented the 16-B<sub>1</sub>-PhytoP-dependent increase in the percentage of O<sub>4</sub>-immunopositive cells. To further support the involvement of PPAR-γ, we evaluated the nuclear translocation of the receptor known to be induced upon

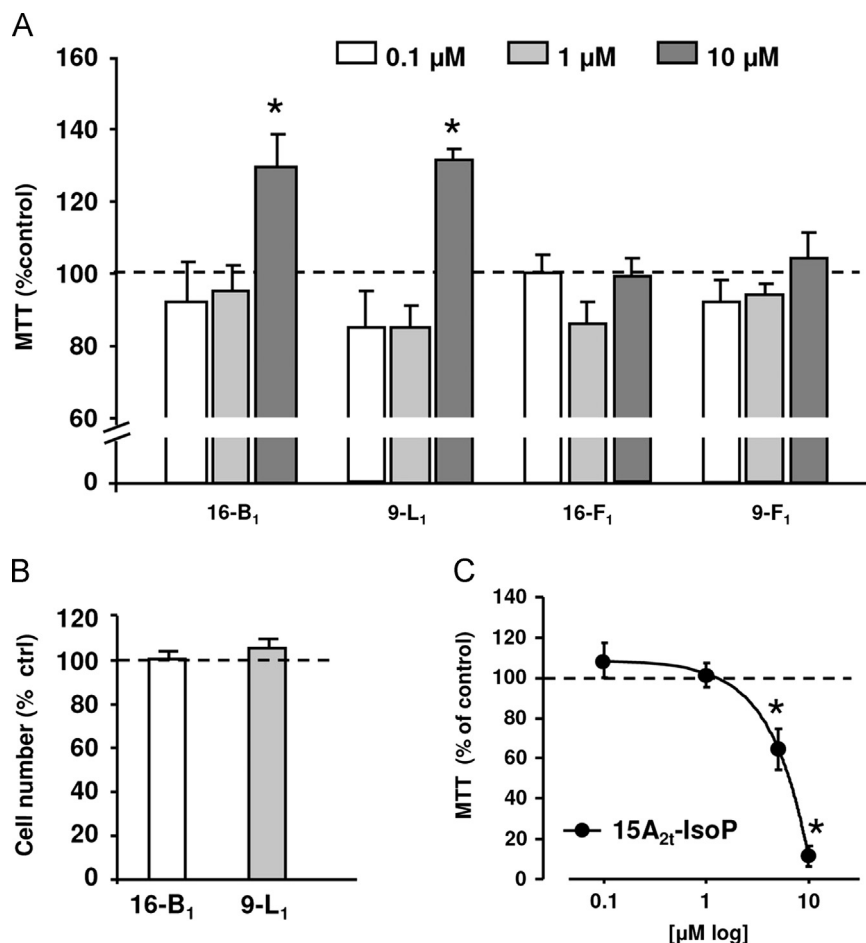


**Fig. 2.** Effects of B<sub>1</sub>- and F<sub>1</sub>-PhytoP's on SH-SY5Y cells. (A) Cell viability of SH-SY5Y cells after 24 h treatment with 0–10 μM PhytoP's, determined by MTT assay. Data are expressed as the percentage of MTT reduction in untreated control cultures. (B) Cell number in cultures after 24 h treatment with 10 μM 16-B<sub>1</sub> and 9-L<sub>1</sub>, determined by CV assay and expressed as a percentage of untreated control cultures (dashed line). (C) Cell viability of SH-SY5Y cells after 24 h treatment with increasing concentrations of the cyclopentenone isoprostane 15-A<sub>21</sub>-IsoP, determined by MTT assay and expressed as a percentage of untreated control cultures (dashed line). Data are the mean ± SEM, from n = 4–8 independent experiments. \*p < 0.05 versus control cultures.

interaction of PPAR- $\gamma$  with the ligand. Fig. 8E shows that PPAR- $\gamma$  immunoreactivity was mainly localized to the nucleus only when cells were exposed to 1  $\mu$ M 16-B<sub>1</sub>-PhytoP, and not the biologically inactive *ent*-9-L<sub>1</sub> PhytoP.

## Discussion

In this study we have shown that B<sub>1</sub>-PhytoP's are biologically active in experimental models of immature cells of the central nervous system. In particular, we tested the activities of the two B<sub>1</sub>-PhytoP regioisomers (16-B<sub>1</sub> and 9-L<sub>1</sub>) and found that they were equally effective in increasing the metabolic activity of SH-SY5Y

cells, used for modeling an early neuronal differentiation stage. In contrast, the two F<sub>1</sub>-PhytoP regioisomers (16-F<sub>1</sub> and 9-F<sub>1</sub>) had no activity on these cells. Because the structural difference between B<sub>1</sub>- and F<sub>1</sub>-PhytoP's lies in their ring, this observation suggests that the cyclopentenone ring in B<sub>1</sub>-PhytoP's, but not the cyclopentane ring in F<sub>1</sub>-PhytoP's, is important for such activity. However, the cyclopentenone 15-A<sub>2</sub>-IsoP, at the same concentration range, was very effective in inducing neuronal cell death, as previously described [17], thus indicating that other structural regions of B<sub>1</sub>-PhytoP's contribute to their biological profile and that compounds generated through analogous nonenzymatic free radical-catalyzed pathways from ALA or AA are endowed with opposite biological activities.

The relation between biological activity and chemical structure was further investigated by testing on SH-SY5Y cells a panel of compounds comprising 16-B<sub>1</sub>-PhytoP and 9-L<sub>1</sub>-PhytoP enantiomers and two B<sub>1</sub>-PhytoP derivatives characterized by a short side chain and alternative allylic alcohol migration. Of the whole panel, only the 16-B<sub>1</sub>-PhytoP enantiomer (*ent*-16-B<sub>1</sub>-PhytoP) retained the activity, suggesting that the allylic configuration and the position of the carboxyl group with respect to the cyclopentenone ring are two additional important factors controlling B<sub>1</sub>-PhytoP bioactivity.

The next aim of our study was to investigate whether the B<sub>1</sub>-PhytoP-induced increase in SH-SY5Y metabolic activity could result in cell protection against oxidant damage. For these experiments, SH-SY5Y cells were exposed to H<sub>2</sub>O<sub>2</sub> at a concentration reducing their metabolic activity by about 50% to fully appreciate any protective or detrimental effect of B<sub>1</sub>-PhytoP's. We found that 16-B<sub>1</sub>-PhytoP, 9-L<sub>1</sub>-PhytoP, and *ent*-16-B<sub>1</sub>-PhytoP fully protected cells from H<sub>2</sub>O<sub>2</sub> damage, whereas *ent*-9-L<sub>1</sub>-PhytoP was devoid of activity, thus confirming the role of allylic configuration in B<sub>1</sub>-PhytoP bioactivity. The lack of protection by *ent*-9-L<sub>1</sub>-PhytoP against H<sub>2</sub>O<sub>2</sub> also ruled out the hypothesis that neuroprotection observed with the other three compounds could be due to a direct scavenging effect of tetrasubstituted cyclopentenone B<sub>1</sub>-PhytoP's.

Interestingly, B<sub>1</sub>-PhytoP's had no effect on differentiated SH-SY5Y cells, either on their metabolic activity or against H<sub>2</sub>O<sub>2</sub>-induced damage. Furthermore, B<sub>1</sub>-PhytoP's did not protect OP cultures from H<sub>2</sub>O<sub>2</sub>-induced damage, but increased their metabolic activity and promoted OP differentiation to OLs, suggesting that the biological activity of these compounds is dependent on the cell type and on their state of differentiation.

To gain some insights into the molecular mechanisms triggered by B<sub>1</sub>-PhytoP in SH-SY5Y cells we focused on the nuclear receptor PPAR- $\gamma$ , a ligand-dependent transcription factor involved in the control of several important functions such as metabolism homeostasis,

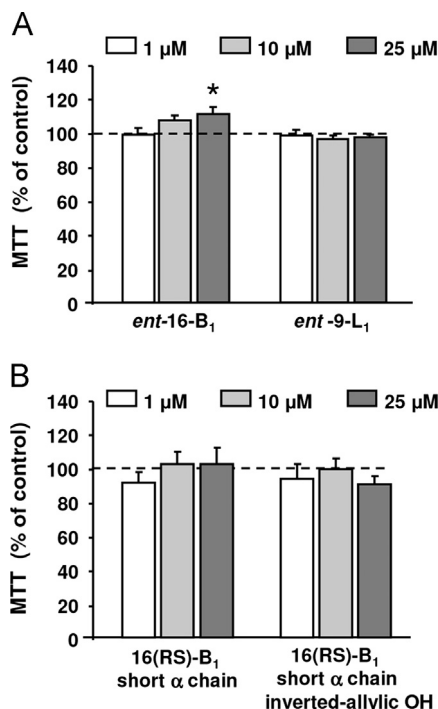


**Fig. 3.** Effects of B<sub>1</sub>-PhytoP enantiomers and derivatives on SH-SY5Y cells. Cell viability of SH-SY5Y cells after 24 h treatment with 0–25  $\mu$ M (A) *ent*-16-B<sub>1</sub> or *ent*-9-L<sub>1</sub> or (B) B<sub>1</sub>-PhytoP derivatives with short  $\alpha$ -chain with alternative allylic alcohol migration, indicated as 16(RS)-B<sub>1</sub> short chain and 16(RS)-B<sub>1</sub> short chain inverted allylic-OH, respectively. Data are expressed as a percentage of MTT reduction in untreated control cultures (ctr);  $n = 4$  independent experiments; \* $p < 0.05$  versus control cultures.

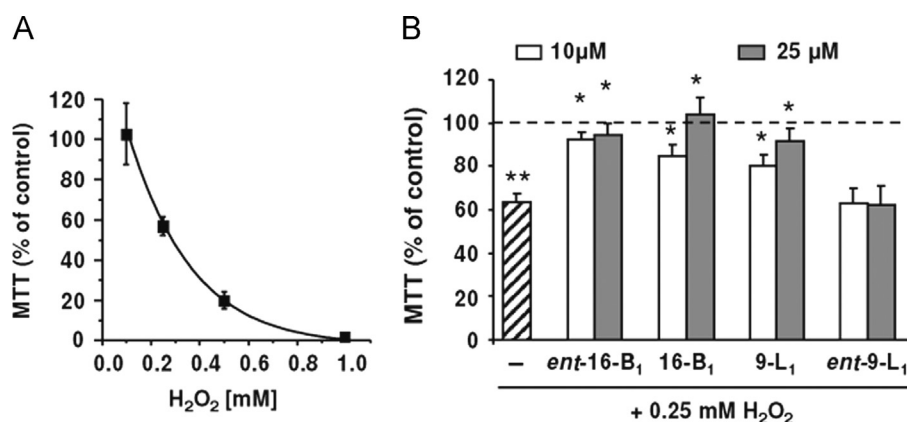


**Fig. 4.** Effects of B<sub>1</sub>-PhytoP's on oxidant injury in SH-SY5Y cells. (A) Cell viability of SH-SY5Y cells after 24 h treatment with increasing H<sub>2</sub>O<sub>2</sub> concentrations, determined by MTT assay. (B) Cell viability of SH-SY5Y cells exposed for 24 h to 0.25  $\mu$ M H<sub>2</sub>O<sub>2</sub>, alone or in combination with 10  $\mu$ M 16-B<sub>1</sub> or 9-L<sub>1</sub> or their enantiomer *ent*-16-B<sub>1</sub> or *ent*-9-L<sub>1</sub>, determined by MTT assay and compared to control cultures. Data are the mean  $\pm$  SEM, from  $n = 4$ –6 independent experiments. \* $p < 0.05$  versus H<sub>2</sub>O<sub>2</sub>-treated cultures; \*\* $p < 0.05$  versus untreated control cultures (dashed line).

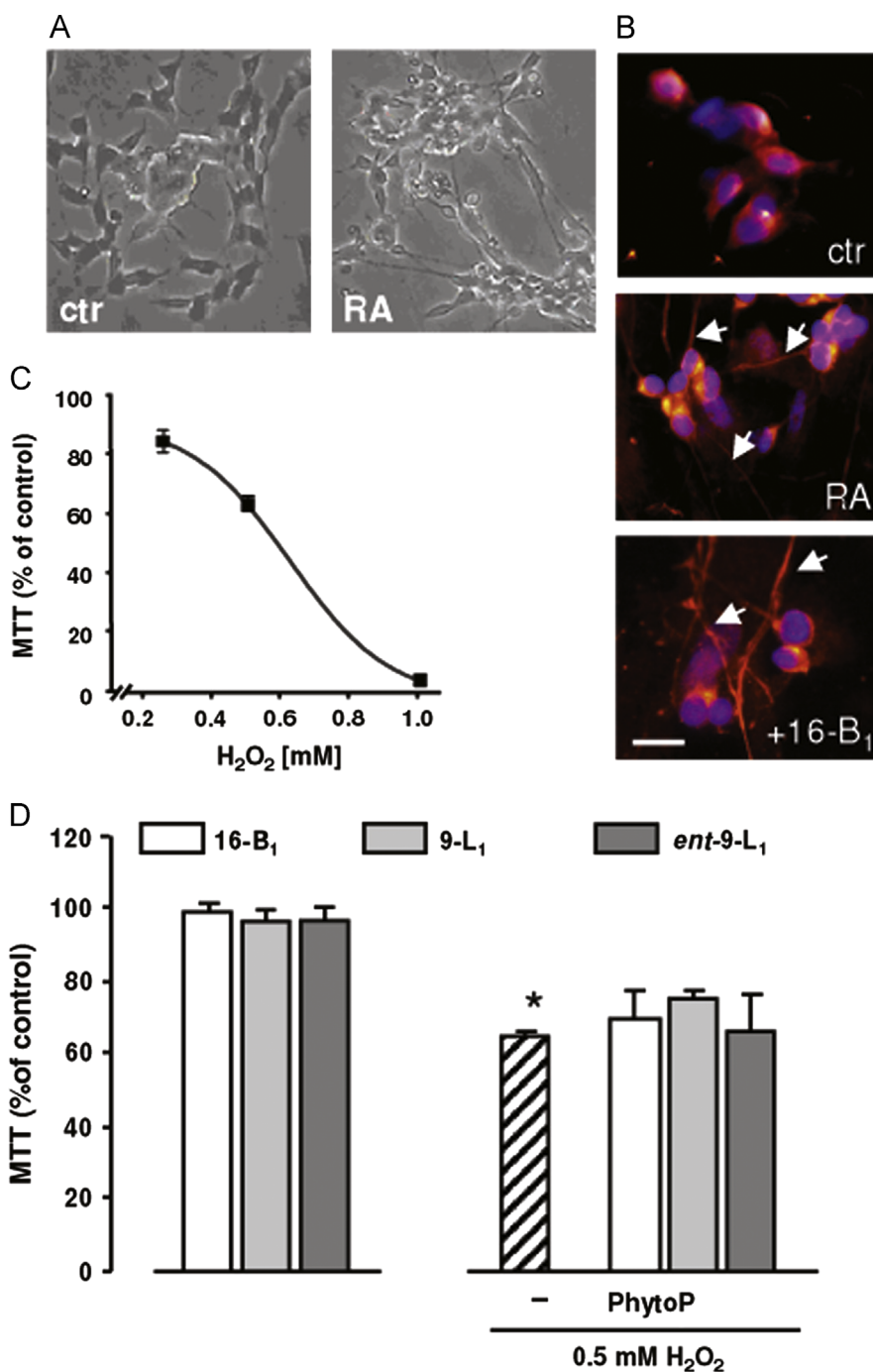


**Fig. 5.** Differentiated SH-SY5Y cells are resistant to B<sub>1</sub>-PhytoP activities. (A) Bright-field images of cells cultured for 5 days in the absence (ctr) or in the presence of retinoic acid (RA), added at day 1 and day 3 as described under Materials and methods. (B) High-magnification images of nuclear stain by Hoechst and MAP2 immunostaining in control and RA-treated cells. Arrows indicate expression of MAP in neurites of differentiated cells. MAP2 expression and neurites were even more pronounced in RA-treated cells receiving 10  $\mu$ M 16-B<sub>1</sub> for the last 24 h. Scale bar, 50  $\mu$ m. (C) Cell viability of differentiated SH-SY5Y cells after 24 h treatment with increasing H<sub>2</sub>O<sub>2</sub> concentrations, determined by MTT assay. (D) Cell viability of differentiated SH-SY5Y cells after 24 h treatment with 10  $\mu$ M 16-B<sub>1</sub>, 9-L<sub>1</sub>, or *ent*-9L<sub>1</sub> (left) or exposed to 0.5 mM H<sub>2</sub>O<sub>2</sub> alone or in combination with 10  $\mu$ M 16-B<sub>1</sub>, 9-L<sub>1</sub>, or *ent*-9L<sub>1</sub>, determined by MTT assay and compared to differentiated control cultures. Data are the mean  $\pm$  SEM, from  $n = 4$  independent experiments. \* $p < 0.05$  versus untreated control cultures.

inflammation, immunity, and cell differentiation [21]. A broad range of structurally different compounds have been shown to activate PPAR- $\gamma$ , most likely because the large ligand-binding cavity allows a relatively free nonspecific interaction with the ligand. Several of the natural compounds with PPAR- $\gamma$  agonistic activity are dietary lipids and their oxidized derivatives, which exhibit higher binding affinity than the unoxidized counterparts [22]. Of interest for our study, ALA has been

shown to stimulate PPAR- $\gamma$  at concentrations ranging from 20 to 100  $\mu$ M in human renal cell carcinoma and monocytic cell lines [23,24], whereas E<sub>1</sub>-PhytoP triggers PPAR- $\gamma$  activation at a concentration as low as 1  $\mu$ M in human dendritic cells [12]. In our study, the presence of the PPAR- $\gamma$  antagonist GW9662 abolished the effects of 16-B<sub>1</sub>-PhytoP, indicating the ability of the compound to trigger PPAR- $\gamma$  activation at 1–10  $\mu$ M concentrations in both neuronal SH-SY5Y cells

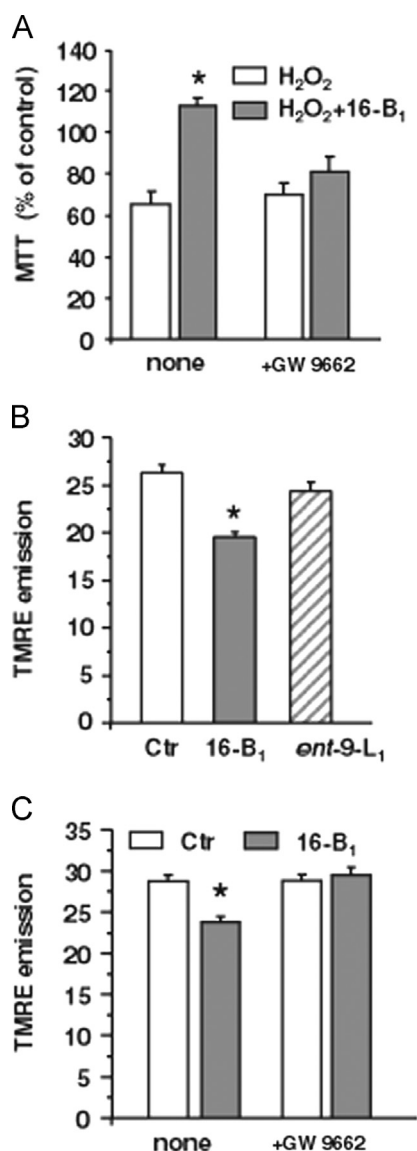


**Fig. 6.** PPAR- $\gamma$  activation is necessary for 16-B<sub>1</sub>-PhytoP activities on SH-SY5Y cells. (A) Cell viability of SH-SY5Y cells exposed for 24 h to 0.25  $\mu$ M H<sub>2</sub>O<sub>2</sub> alone or in combination with 10  $\mu$ M 16-B<sub>1</sub>, in the absence or in the presence of the PPAR- $\gamma$  antagonist GW9662 (1  $\mu$ M), determined by MTT assay and compared to control cultures. Data are the mean  $\pm$  SEM, from  $n = 3$  independent experiments; \* $p < 0.05$  versus H<sub>2</sub>O<sub>2</sub>-treated cultures. (B) Mitochondrial membrane potential (mMP) in cultures exposed to 10  $\mu$ M 16-B<sub>1</sub> or *ent-9-L<sub>1</sub>* for 24 h; mMP was measured by using the potentiometric dye TMRE in single-cell video-imaging experiments. Data are the mean  $\pm$  SEM, expressed as arbitrary units, from  $n = 3$  independent experiments; \* $p < 0.05$  versus control cultures. (C) mMP in cultures exposed to 10  $\mu$ M 16-B<sub>1</sub> alone or in combination with the PPAR- $\gamma$  antagonist GW9662, measured as in (B). Data are the mean  $\pm$  SEM, from  $n = 3$  independent experiments; \* $p < 0.05$  versus control cultures.

and OP cultures. The activation of PPAR- $\gamma$  is further indicated by its nuclear translocation upon stimulation with 16-B<sub>1</sub>-PhytoP but not the biologically inactive *ent-9-L<sub>1</sub>*-PhytoP.

Both SH-SY5Y cells and OPs constitutively express PPAR- $\gamma$ . In line with our results, PPAR- $\gamma$  agonists (pioglitazone and 15d-PGJ<sub>2</sub>) prevented the death of differentiated SH-SY5Y cells exposed to transient glucose deprivation [25] and promoted OP differentiation [14,26].

In the search for a mechanism of protection against H<sub>2</sub>O<sub>2</sub> in SH-SY5Y cells, we did not find any effect of B<sub>1</sub>-PhytoP on the expression of genes involved in free radical scavenging, such as

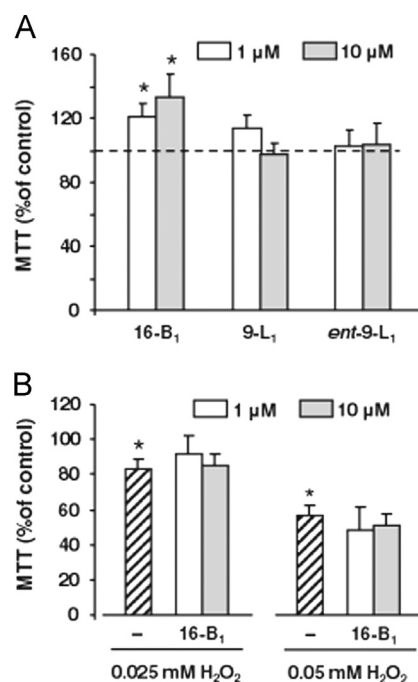


**Fig. 7.** Effects of B<sub>1</sub>-PhytoPs on oligodendrocyte progenitors. (A) Cell viability of OPs after 24 h treatment with 10  $\mu$ M 16-B<sub>1</sub>, 9-L<sub>1</sub>, or *ent-9-L<sub>1</sub>*, determined by MTT assay. (B) Cell viability of OP cultures exposed for 24 h to 25 or 50  $\mu$ M H<sub>2</sub>O<sub>2</sub> alone or in combination with 1 or 10  $\mu$ M 16-B<sub>1</sub>, determined by MTT assay and compared to control cultures. Data presented in (A) and (B) are expressed as percentage of control cultures and are the mean  $\pm$  SEM, from  $n = 4-6$  independent experiments; \* $p < 0.05$  versus untreated control cultures.

catalase or Cu/Zn- and Mn-superoxide dismutases, but we observed a moderate reduction in the mMP, an effect that was prevented by GW9662. A slight degree of depolarization within the inner membrane of mitochondria might play a protective role by attenuating the production of reactive oxygen species (ROS) by these organelles, thus rendering cells more fit to face an oxidant injury [20]. Depolarization of the inner membrane, reduced ROS production, and protection from brief anoxia-reoxygenation have been reported in isolated heart mitochondria of mice receiving a 3-week diet enriched with pioglitazone [27]. Interestingly, this study demonstrated that the effects of pioglitazone are related to the increased expression of the mitochondrial protein UCP-2, known to be under the control of PPARs [27]. It can be envisaged that a similar protection could occur in B<sub>1</sub>-PhytoP-treated SH-SY5Y neuroblasts exposed to H<sub>2</sub>O<sub>2</sub>. SH-SY5Y cells are widely used to study oxidative stress-induced cell damage: the molecular mechanisms triggered by H<sub>2</sub>O<sub>2</sub> or other toxic agents are complex and specific for undifferentiated or RA-differentiated cells [16,28]. In particular, the mitochondrial response seems different in neuroblasts and RA-differentiated cells; as an example, mitochondrial depolarization was faster and more pronounced in undifferentiated SH-SY5Y than in RA-differentiated cells exposed to 6-hydroxydopamine, suggesting that neuronal cells acquire mitochondria-protective mechanisms during differentiation [28]. This would explain the ability of B<sub>1</sub>-PhytoPs to protect undifferentiated but not RA-differentiated SH-SY5Y cells. Along this line, it is interesting to note that pioglitazone did not affect mMP in differentiated SH-SY5Y cells [25]. Furthermore, 16-B<sub>1</sub>-PhytoP added to differentiating SH-SY5Y cells (at 4 DIV) accelerated the formation of neurites, as previously described for the PPAR- $\gamma$  agonist pioglitazone [19].

In OP cultures the lack of protection against a mild to moderate H<sub>2</sub>O<sub>2</sub> damage could be related to the nonsignificant effect on mMP. In agreement with these results, we have previously shown that

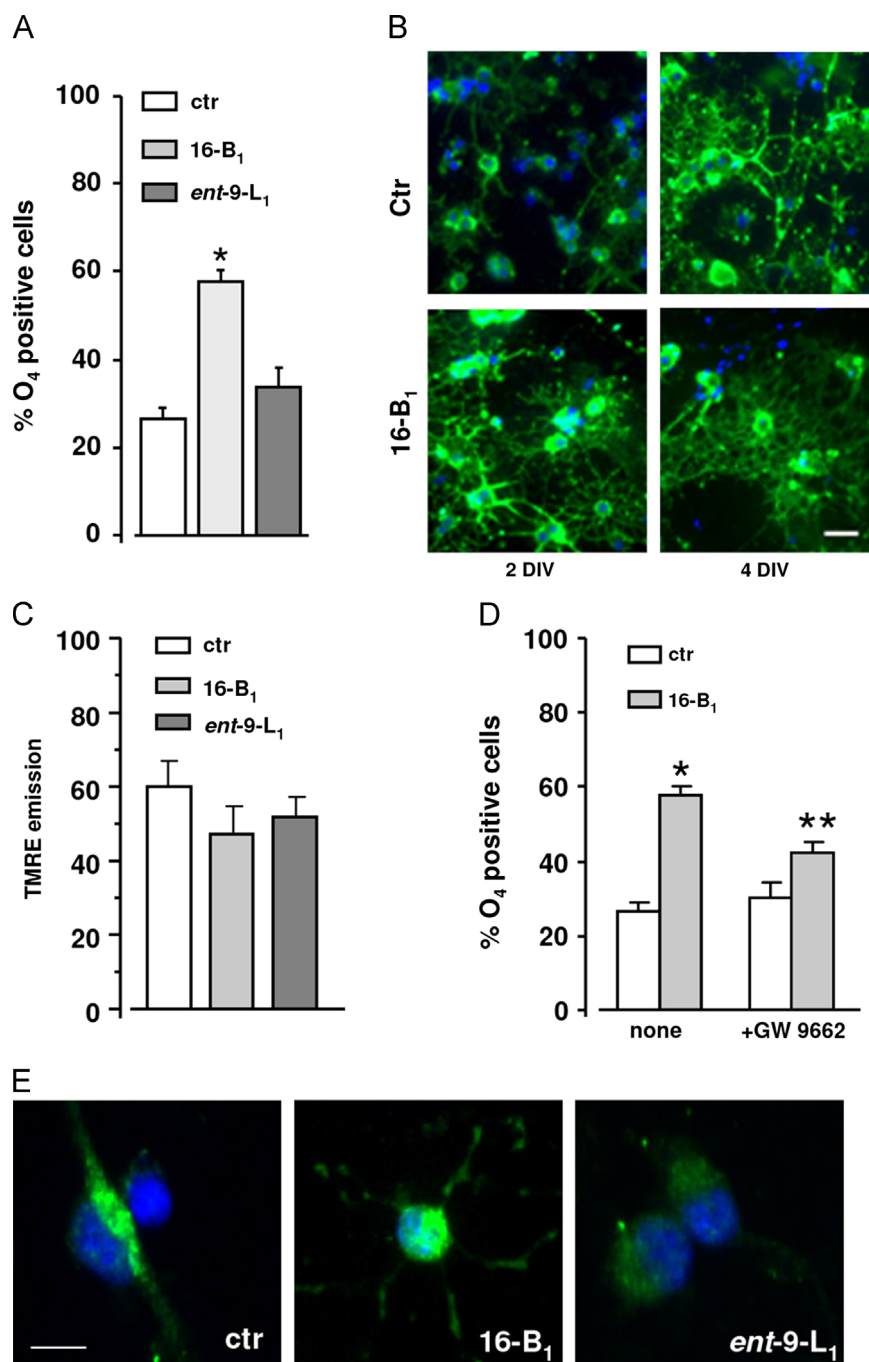


**Fig. 8.** 16-B<sub>1</sub>-Phyto induces oligodendrocyte differentiation through mechanisms involving PPAR- $\gamma$  activation. (A) OP cultures were treated for 24 h with 1  $\mu$ M 16-B<sub>1</sub> or *ent-9-L<sub>1</sub>*. OP differentiation to immature OLs was determined by evaluating the percentage of cells expressing O<sub>4</sub>, a typical marker for this OL developmental stage. Nuclei were stained using Hoechst 33258. Data are given as the percentage of positive cells over the total cell number under each condition and are the mean  $\pm$  SEM from  $n = 4$  independent experiments; \* $p < 0.05$  versus untreated control cultures and versus *ent-9-L<sub>1</sub>*-treated cultures. (B) Images of Hoechst 33258 nuclear staining (blue) and O<sub>4</sub> immunostaining (green) in cultures grown for 24 h (2 DIV) or 72 h (4 DIV) under control (Ctr; top) and 16-B<sub>1</sub>-treated (bottom) conditions. Images show the more complex morphology of 16-B<sub>1</sub>-treated cells, indicating a more mature developmental stage. Scale bar, 50  $\mu$ m. (C) Mitochondrial membrane potential in cultures exposed to 10  $\mu$ M 16-B<sub>1</sub> or *ent-9-L<sub>1</sub>* for 24 h; mMP was measured by using the potentiometric dye TMRE in single-cell video-imaging experiments. Data are the mean  $\pm$  SEM and are expressed as arbitrary units;  $n = 4$  independent experiments. (D) Percentage of O<sub>4</sub>-positive cells in cultures treated for 24 h with 1  $\mu$ M 16-B<sub>1</sub> alone or in the presence the PPAR- $\gamma$  antagonist GW9662 (1  $\mu$ M). Data are the mean  $\pm$  SEM from  $n = 4$  independent experiments; \* $p < 0.05$  versus untreated control cultures; \*\* $p < 0.05$  versus 16-B<sub>1</sub>-treated cultures. (E) Images of Hoechst 33258 nuclear staining (blue) and PPAR- $\gamma$  immunostaining (green) in cultures grown for 24 h in the absence (ctr) or in the presence of 1  $\mu$ M 16-B<sub>1</sub> or *ent-9-L<sub>1</sub>*. Images show PPAR- $\gamma$  nuclear localization only in cultures exposed to 16-B<sub>1</sub>. Scale bar, 50  $\mu$ m. (For interpretation of the references to color in this figure legend, the reader is referred to the web version of this article.)

PPAR- $\gamma$  agonists do not influence mMP in OL cultures, although they accelerate OP differentiation to OLs through a mechanism involving mitochondrial functions, such as the mitochondrial respiratory chain activity and oscillatory Ca<sup>2+</sup> wave regulation [26].

Altogether, these observations suggest that B<sub>1</sub>-PhytoP bioactivities are cell-type-dependent and restricted to immature cells.

Indeed, we have shown that B<sub>1</sub>-PhytoP's, through mechanisms involving PPAR- $\gamma$ , can affect neuroblasts and OPs thereby conferring neuroprotection against oxidant injury and promoting myelination, respectively. Being dietary components, PhytoP's should be included in the large group of nutraceuticals that can activate PPAR- $\gamma$  and that could be exploited to promote health benefits

[22]. In the past decade, there has been an increasing interest in the anti-inflammatory and neuroprotective activities of PPAR- $\gamma$  agonists and their therapeutic potential in a variety of brain disorders [21,29,30]. Nonetheless, the toxicity associated with some synthetic agonists, including the antidiabetic glitazones, has fostered the search for alternative strategies for targeting PPAR- $\gamma$ . In particular, there has been an increasing interest in natural compounds that can be integrated into the daily diet and provide a complementary treatment for chronic diseases including neurological diseases such as multiple sclerosis [31].

Finally, the high content of PhytoP's in pollen suggests that these molecules can gain access to the brain through the nasal mucosa, via the olfactory epithelium, which represents a direct route from the nose to the brain along the olfactory and trigeminal nerve pathways, or via the vascular route into the blood and across the blood-brain barrier [32]. Through these routes B<sub>1</sub>-PhytoP's could reach brain areas in which stem and progenitor cells reside and influence their fate.

Our study highlights the importance of a detailed knowledge of the biological activities of PhytoP's in mammalian systems to appreciate the potential benefit and detriment of accidental (pollen) or deliberate (diet and parenteral lipid nutrition) exposure to these oxidized lipids.

## Acknowledgments

This work was supported by the Istituto Superiore di Sanità, CNRS, and University Montpellier I. The technical assistance of Claudio Di Giuseppe is gratefully acknowledged.

## References

- [1] Roberts 2nd L. J.; Fessel, J. P.; Davies, S. S. The biochemistry of the isoprostane, neuroprostane, and isofuran pathways of lipid peroxidation. *Brain Pathol.* **15**:143–148; 2005.
- [2] Galano, J. M.; Mas, E.; Barden, A.; Mori, T. A.; Signorini, C.; De Felice, C.; Barrett, A.; Opere, C.; Pinot, E.; Schwedhelm, E.; Benndorf, R.; Roy, J.; Le Guennec, J. Y.; Oger, C.; Durand, T. Isoprostanes and neuroprostanes: total synthesis, biological activity and biomarkers of oxidative stress in humans. *Prostaglandins Other Lipid Mediators* **107**:95–102; 2013.
- [3] Durand, T.; Bultel-Poncé, V.; Guy, A.; Berger, S.; Mueller, M. J.; Galano, J. M. New bioactive oxylipins formed by non-enzymatic free-radical-catalyzed pathways: the phytoprostanes. *Lipids* **44**:875–888; 2009.
- [4] Thoma, I.; Krischke, M.; Loeffler, C.; Mueller, M. J. The isoprostanoic pathway in plants. *Chem. Phys. Lipids* **128**:135–148; 2004.
- [5] Jahn, U.; Galano, J. M.; Durand, T. A cautionary note on the correct structure assignment of phytoprostanes and the emergence of a new prostane ring system. *Prostaglandins Leukotrienes Essent. Fatty Acids* **82**:83–86; 2010.
- [6] El Fangour, S.; Guy, V.; Despres, A.; Vidal, J. -C.; Rossi, J. -P.; Durand, T. Total syntheses of the eight diastereoisomers of the syn-anti-syn phytoprostanes F1 types I and II. *J. Org. Chem.* **69**:2498–2503; 2004.
- [7] Pinot, E.; Guy, A.; Fournial, A.; Balas, L.; Rossi, J. C.; Durand, T. Total synthesis of the four enantiomerically pure diastereoisomers of the phytoprostanes E1 type II and of the 15-E2t-isoprostanes. *J. Org. Chem.* **73**:3063–3069; 2008.
- [8] Durand, T.; Bultel-Poncé, V.; Guy, A.; El Fangour, S.; Rossi, J. C.; Galano, J. M. Isoprostanes and phytoprostanes: bioactive lipids. *Biochimie* **93**:52–60; 2011.
- [9] Karg, K.; Dirsch, V. M.; Vollmar, A. M.; Cracowski, J. L.; Laporte, F.; Mueller, M. J. Biologically active oxidized lipids (phytoprostanes) in the plant diet and parenteral lipid nutrition. *Free Radic. Res.* **41**:25–37; 2007.
- [10] Barden, A. E.; Croft, K. D.; Durand, T.; Guy, A.; Mueller, M. J.; Mori, T. A. Flaxseed oil supplementation increases plasma F<sub>1</sub>-phytoprostanes in healthy men. *J. Nutr.* **139**:1890–1895; 2009.
- [11] Traidl-Hoffmann, C.; Mariani, V.; Hochrein, H.; Karg, K.; Wagner, H.; Ring, J.; Mueller, M. J.; Jakob, T.; Behrendt, H. Pollen-associated phytoprostanes inhibit dendritic cell interleukin-12 production and augment T helper type 2 cell polarization. *J. Exp. Med.* **201**:627–636; 2005.
- [12] Gilles, S.; Mariani, V.; Bryce, M.; Mueller, M. J.; Ring, J.; Jakob, T.; Pastore, S.; Behrendt, H.; Traidl-Hoffmann, C. Pollen-derived E1-phytoprostanes signal via PPAR-gamma and NF-kappaB-dependent mechanisms. *J. Immunol.* **182**:6653–6658; 2009.
- [13] Biedler, J. L.; Roffler-Tarlov, S.; Schachner, M.; Freedman, L. S. Multiple neurotransmitter synthesis by human neuroblastoma cell lines and clones. *Cancer Res.* **38**:3751–3758; 1978.
- [14] Bernardo, A.; Bianchi, D.; Magnaghi, V.; Minghetti, L. Peroxisome proliferator-activated receptor-gamma agonists promote differentiation and antioxidant defenses of oligodendrocyte progenitor cells. *J. Neuropathol. Exp. Neurol.* **68**:797–808; 2009.
- [15] El Fangour, S.; Guy, A.; Vidalm, J. -P.; Rossi, J. -C.; Durand, T. A flexible synthesis of the phytoprostanes B1 types I and II. *J. Org. Chem.* **70**:989–997; 2005.
- [16] Ruffels, J.; Griffin, M.; Dickenson, J. M. Activation of ERK1/2, JNK and PKB by hydrogen peroxide in human SH-SY5Y neuroblastoma cells: role of ERK1/2 in H<sub>2</sub>O<sub>2</sub>-induced cell death. *Eur. J. Pharmacol.* **483**:163–173; 2004.
- [17] Musiek, E. S.; Breeding, R. S.; Milne, G. L.; Zannoni, G.; Morrow, J. D.; McLaughlin, B. Cyclopentenone isoprostanes are novel bioactive products of lipid oxidation which enhance neurodegeneration. *J. Neurochem.* **97**:1301–1313; 2006.
- [18] Xie, H. R.; Hu, L. S.; Li, G. Y. SH-SY5Y human neuroblastoma cell line: in vitro cell model of dopaminergic neurons in Parkinson's disease. *Chin. Med. J. (English ed.)* **123**:1086–1092; 2010.
- [19] Miglio, G.; Rattazzi, L.; Rosa, A. C.; Fantozzi, R. PPARgamma stimulation promotes neurite outgrowth in SH-SY5Y human neuroblastoma cells. *Neurosci. Lett.* **454**:134–138; 2009.
- [20] Brookes, P. S. Mitochondrial H<sup>+</sup> leak and ROS generation: an odd couple. *Free Radic. Biol. Med.* **38**:12–23; 2005.
- [21] Bernardo, A.; De Simone, R.; De Nuccio, C.; Visentin, S.; Minghetti, L. The nuclear receptor peroxisome proliferator-activated receptor- $\gamma$  promotes oligodendrocyte differentiation through mechanisms involving mitochondria and oscillatory Ca<sup>2+</sup> waves. *Biol. Chem.* **394**:1607–1614; 2013.
- [22] Penumetcha, M.; Santanam, N. Nutraceuticals as ligands of PPAR $\gamma$ . *PPAR Res.* **2012**:858352; 2012.
- [23] Yang, L.; Yuan, J.; Liu, L.; Shi, C.; Wang, L.; Tian, F.; Liu, F.; Wang, H.; Shao, C.; Zhang, Q.; Chen, Z.; Qin, W.; Wen, W.  $\alpha$ -Linolenic acid inhibits human renal cell carcinoma cell proliferation through PPAR- $\gamma$  activation and COX-2 inhibition. *Oncol. Lett.* **6**:197–202; 2013.
- [24] Zhao, G.; Etherton, T. D.; Martin, K. R.; Vanden Heuvel, J. P.; Gillies, P. J.; West, S. G.; Kris-Etherton, P. M. Anti-inflammatory effects of polyunsaturated fatty acids in THP-1 cells. *Biochem. Biophys. Res. Commun.* **336**:909–917; 2005.
- [25] Miglio, G.; Rosa, A. C.; Rattazzi, L.; Collino, M.; Lombardi, G.; Fantozzi, R. PPARgamma stimulation promotes mitochondrial biogenesis and prevents glucose deprivation-induced neuronal cell loss. *Neurochem. Int.* **55**:496–504; 2009.
- [26] De Nuccio, C.; Bernardo, A.; De Simone, R.; Mancuso, E.; Magnaghi, V.; Visentin, S.; Minghetti, L. Peroxisome proliferator-activated receptor  $\gamma$  agonists accelerate oligodendrocyte maturation and influence mitochondrial functions and oscillatory Ca(2+) waves. *J. Neuropathol. Exp. Neurol.* **70**:900–912; 2011.
- [27] Cabrera, J. A.; Ziemba, E. A.; Colbert, R.; Kelly, R. F.; Kuskowski, M.; Arriaga, E. A.; Sluiter, W.; Duncker, D. J.; Ward, H. B.; McFalls, E. O. Uncoupling protein-2 expression and effects on mitochondrial membrane potential and oxidant stress in heart tissue. *Transl. Res.* **159**:383–390; 2012.
- [28] Lopes, F. M.; Schroder, R.; da Frota Jr M. L.; Zanutto-Filho, A.; Müller, C. B.; Pires, A. S.; Meurer, R. T.; Colpo, G. D.; Gelain, D. P.; Kapczinski, F.; Moreira, J. C.; Fernandes, C.; Klamt, F. Comparison between proliferative and neuron-like SH-SY5Y cells as an in vitro model for Parkinson disease studies. *Brain Res.* **1337**:85–94; 2010.
- [29] Heneka, M. T.; Landreth, G. E.; Hüll, M. Drug insight: effects mediated by peroxisome proliferator-activated receptor-gamma in CNS disorders. *Nat. Clin. Pract. Neurol.* **3**:496–504; 2007.
- [30] Bernardo, A.; Minghetti, L. Regulation of glial cell functions by PPAR-gamma natural and synthetic agonists. *PPAR Res.* **2008**:864140; 2008.
- [31] Riccio, P. The molecular basis of nutritional intervention in multiple sclerosis: a narrative review. *Complement Ther. Med.* **19**:228–237; 2011.
- [32] Dhuria, S. V.; Hanson, L. R.; Frey 2nd W. H. Intranasal delivery to the central nervous system: mechanisms and experimental considerations. *J. Pharm. Sci.* **99**:1654–1673; 2010.